Journal of Alloys and Compounds 509 (2011) L137–L141

Contents lists available at ScienceDirect

Journal of Alloys and Compounds

journal homepage: www.elsevier.com/locate/jallcom

Letter

Micro-arc oxidation of TC4 substrates to fabricate TiO_2/YAG:Ce^{3+} compound films with enhanced photocatalytic activity

Xudong Jiang[a], Yongqian Wang[a,b], Chunxu Pan[a,*]

[a] Department of Physics and Key Laboratory of Acoustic and Photonic Materials and Devices of Ministry of Education, Wuhan University, Luo Jia Shan, Wuchang, Wuhan 430072, Hubei, China

[b] Engineering Research Center of Nano-Geomaterials of Ministry of Education, China University of Geosciences, Wuhan 430074, China

ARTICLE INFO

Article history:
Received 6 August 2010
Received in revised form
16 December 2010
Accepted 17 December 2010
Available online 24 December 2010

Keywords:
TiO_2 photocatalytic film
YAG:Ce^{3+} semiconductor
Micro-arc oxidation
Compounded film

ABSTRACT

This paper introduces a process for "*in situ*" preparing TiO_2 photocatalytic film compounded with YAG:Ce^{3+} semiconductor upon titanium alloy by using micro-arc oxidation (MAO). The surface morphology, chemical compositions, phase structures and photocatalytic properties of the films were characterized and measured by field emission gun scanning electron microscope (FEG-SEM), energy-dispersive X-ray spectrometer (EDS), X-ray diffractometer (XRD), electro-chemical workstation and UV–vis spectrophotometer. The results show that the YAG:Ce^{3+} semiconductor particles which were added in the electrolyte had been homogenously compounded within the TiO_2 film during MAO. Compared with the pure TiO_2 film, the compounded film exhibited much larger specific surface area, stronger absorption in the visible light and higher photo-generated current density, which improves the photocatalytic property markedly. It is expected that MAO will provide a simple, economic and promising approach for preparing a superior photocatalytic TiO_2 film.

1. Introduction

Since the report about photolysis of water on titanium dioxide (TiO_2) by Fujishima and Honda in 1972 [1], TiO_2 has been extensively studied due to its chemical stability, biological compatibility and anti-photo-corrosion ability. However, TiO_2 powder is hard to be recycled in polluted water and the depth of photo-radiation is limited. TiO_2 powder fossilization and the preparation of TiO_2 film have become hot research directions recently [2–4].

It is well known that TiO_2 has higher absorbance in ultraviolet light range due to its large band gap (such as E_g = 3.2 eV for anatase), which indicates only 4% of the sunlight spectrum can be used. In addition, TiO_2 exhibits lower efficiency of photocatalysis because of the recombination of the photo-generated electrons and holes pairs (e^-/h^+) happens easily [5]. Therefore, these two key problems need to be addressed, i.e. expanding the wavelength response range to the visible light range and reducing the recombination rate of charge carriers in TiO_2 film.

Currently, a variety of methods have been employed to improve the photocatalytic property of TiO_2 film, such as: metal doping [6], nonmetal doping [7] and coupling TiO_2 with other semiconductor compound [8]. Generally, metal doping can create electron traps to reduce e^-/h^+ recombination rate and increase the current carriers by replacement of Ti^{4+} came from TiO_2. Nonmetal doping is used for narrowing the band gap of TiO_2, followed by expanding the wavelength response range to visible region. Based on its advantages both on the inhibition of the recombination of e^-/h^+ [9] and the enhancement of the absorption in the visible light, the semiconductor compound is recognized as a promising way to improve the photocatalytic property of TiO_2. Up to now, several processes have been developed to prepare TiO_2 films, such as sol–gel [10], anodic oxidation [11] and magnetron sputtering [12]. However, the film from sol–gel and anodic oxidation exhibit a poor adhesion with substrates, and the film from magnetron sputtering is expensive and only 10–20 nm in thickness.

Micro-arc oxidation (MAO) is a kind of surface treatment through an electrochemical and plasma-chemical process. It provides a possibility for "*in situ*" formation of a ceramic oxide film upon the surface of valve-metal including Al, Mg, Ti and their alloys [13]. The oxide film formed via MAO exhibits good adhesion to substrate, excellent chemical durability, high abradability and high temperature resistance, etc. When Ti or Ti alloys is used as a substrate, an excellent adhesive TiO_2 film will be made on it, and the surface morphology, film thickness and phase structure of the film can be controlled by adjusting the experimental conditions such as electrical parameters [14,15] and electrolyte components [16], for improving its photocatalytic property.

* Corresponding author. Tel.: +86 27 68752481x5201; fax: +86 27 68752569.
E-mail address: cxpan@whu.edu.cn (C. Pan).

0925-8388/$ – see front matter.
doi:10.1016/j.jallcom.2010.12.131

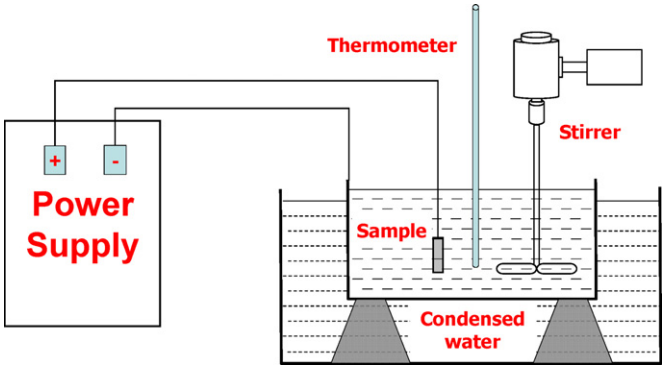

Fig. 1. Schematic diagram of micro-arc oxidation experimental installation.

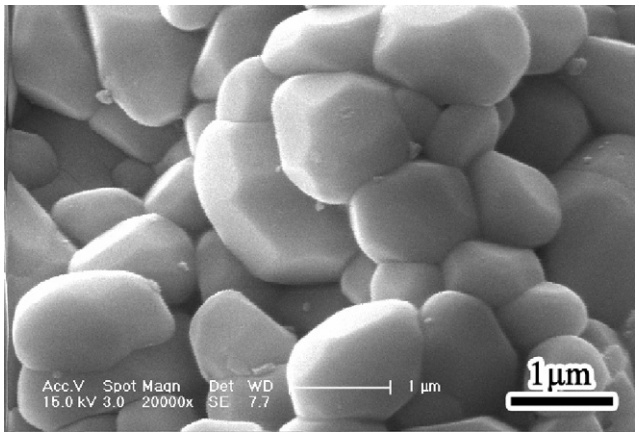

Fig. 2. SEM morphologies of YAG:Ce^{3+} particles.

Yttrium aluminum garnet (YAG, $Y_3Al_5O_{12}$) has been recognized as one of the best phosphor host materials. The radius of Y ion is similar to the trivalent rare-earth Ce^{3+}. Therefore, Ce^{3+} can serve as a catalyst doped into YAG, and exhibits a strong absorbance in the visible light [17]. It has been reported that the dopant of YAG:Er^{3+} could improve nanometer TiO_2 photocatalytic activities [18]. In the present work, a certain quantity of YAG:Ce^{3+} particles was added into the electrolyte during the formation of the TiO_2 film by MAO. Then, the TiO_2/YAG:Ce^{3+} compound film was prepared upon the Ti alloy substrates directly. It is expected to improve the photocatalytic property of the TiO_2 film.

2. Experimental

2.1. YAG:Ce^{3+} preparation

The YAG:Ce^{3+} particles were prepared by high temperature solid state (HTSS) process. The Al_2O_3, Y_2O_3 and CeO_2 powers were mixed in a molar ratio of 25:14:2 and milled for sufficient mixing. Then, the mixture was annealed at 1450 °C for 2 h in hydric deoxidation condition.

2.2. TiO_2 film preparations

Fig. 1 illustrates the schematic diagram of the MAO set-up. The type TC4 (Ti6Al4V) Ti alloy with a size of 2 cm × 2 cm × 0.6 cm was used as an anode. Stainless steel container was selected as an electrolyte cell as well as cathode. The electrolyte solution was consisted of 20 g/L analytical-grade Na_2CO_3 and 8 g/L analytical-grade $Na_2SiO_3{\cdot}9H_2O$. As-synthesized YAG:Ce^{3+} powder was added into the electrolyte. The electrical current was applied by a micro-arc oxidation power supply (PN-III MAO power supply, Institute of plasma technology at South-Central University for Nationalities, China). The experimental conditions were listed in Table 1. The temperature of electrolyte was controlled below 40 °C by condensed water.

2.3. Characterizations

A field emission gun scanning electron microscope (FEG-SEM) (Sirion SEM, FEI, Netherlands) with an energy-dispersive X-ray spectrometer (EDS) was employed to characterize the morphology and chemical compositions. The crystalline structures of the TiO_2 films were examined by using an X-ray diffraction (XRD) spectrometer (D8 Advanced XRD, Bruker AXS, Germany) with Cu Kα source. The scanning speed was 6° per minute. The UV–vis diffuse reflectance spectra (DRS) of the TiO_2 films were measured by using a diffuse reflectance accessory of UV–vis spectrophotometer (UV-2550, Shimadzu, Japan).

2.4. Photo-generated current test

The TiO_2 films, saturation calomel electrode and platinum electrode were worked as the working electrode, reference electrode and counter electrode, respectively. They were all immersed in 1 M NaOH aqueous solution together. The working electrode 4 cm^2 TiO_2 films were irradiated horizontally by 160 W high pressure mercury lamp, which generate light wavelength in the range of 350–450 nm. The distance between the lamp and electrode was 10 cm. The intensity of photo-generated current was measured by electrochemical workstation (CHI660C, Chenhua, Shanghai, China).

2.5. Photo-decomposition test

The photocatalytic activity of the TiO_2 films was measured by the degradation of methyl blue. The TiO_2 films of 4 cm^2 were entirely immersed into 50 mL aqueous methyl blue solution (12 mg/L). The 160 W high pressure mercury lamp was used as a light source irradiated perpendicularly to the film surface. The distance between the lamp and the film was 15 cm. The concentration methyl blue was measured by the UV–vis spectrophotometer (UV-2550, Shimadzu, Japan) every 60 min.

3. Results and discussion

3.1. Microstructural characteristics of the TiO_2/YAG:Ce^{3+} compound film

Fig. 2 shows the morphology of original YAG:Ce^{3+} particles. The shape of particles is polyhedron with edges and corners. The size is around 1–3 μm. Figs. 3 and 4 show the SEM morphologies of pure TiO_2 film and TiO_2 film compounded with the YAG:Ce^{3+} semiconductor, respectively. Obviously, the surface of pure TiO_2 film exhibits typical crater and porous microstructures with a diameter around 1–4 μm. However, in the compounded film, there are many bright particles homogeneously distributed within the film around the micropores, which shows a compact combination with the substrate and no distinct interface. It is also found that the particles became roundish, and the edges and corners in original particles have disappeared, due to the high temperature and short range diffusion at the interface. The chemical compositions of the bright particles arrowed in Fig. 4(b) were identified by using EDS analysis. Besides Na and Si from electrolyte and Ti from substrate, it mainly contains 31.6 at.% Al and 22.65 at.% Y with a few amount of element

Table 1
Experimental conditions of micro-arc oxidation.

Samples	Electrical parameter						Electrolyte	
	Voltage		Frequency	Duty cycle	Time	Na_2CO_3	$Na_2SiO_3{\cdot}9H_2O$	YAG:Ce^{3+}
	Positive	Negative						
TiO_2	300 V	10 V	1 kHz	20%	10 min	20 g/L	8 g/L	–
TiO_2/YAG:Ce^{3+}	300 V	10 V	1 kHz	20%	10 min	20 g/L	8 g/L	2 g/L

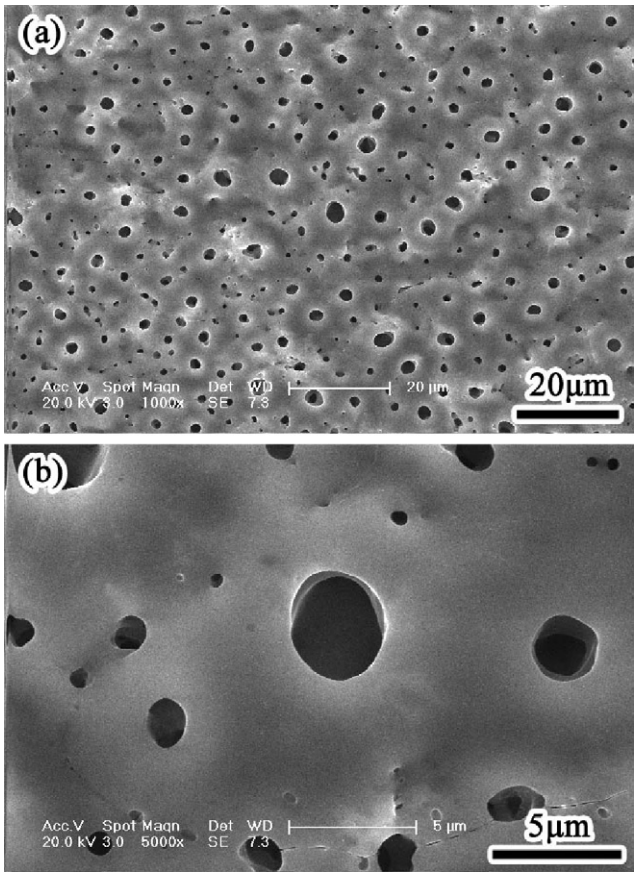

Fig. 3. SEM morphologies of TiO_2 film without composites. (a) Low magnification; (b) high magnification.

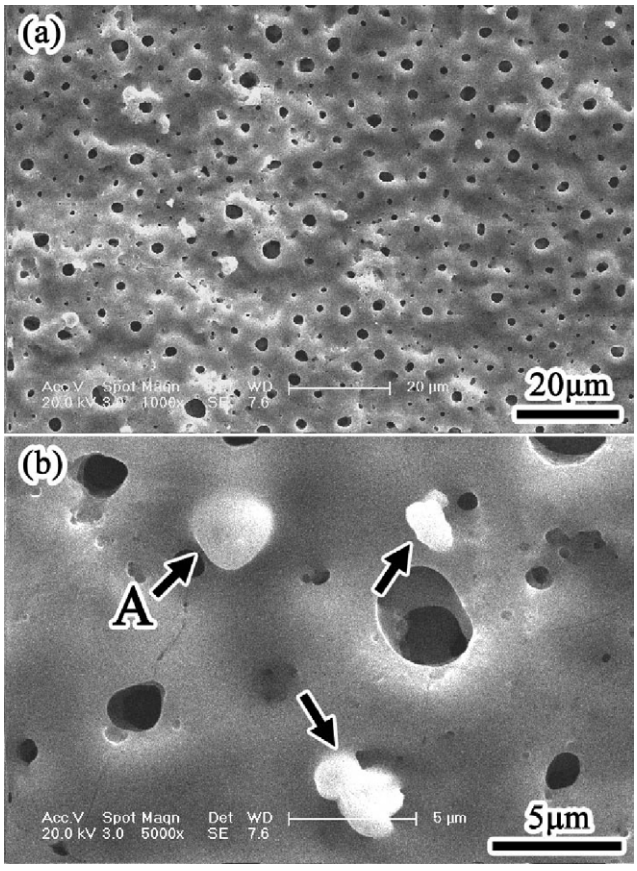

Fig. 4. SEM morphologies of TiO_2 film compounded with the YAG:Ce^{3+}. (a) Low magnification; (b) high magnification (arrows indicate the YAG:Ce^{3+} particles).

Ce, as shown in Fig. 5, which is similar to the chemical compositions of YAG ($Y_3Al_5O_{12}$):Ce^{3+}. Therefore, it is demonstrated that YAG:Ce^{3+} semiconductor has been compounded into the TiO_2 film. About 3% YAG nanoparticles have been incorporated within the TiO_2 film by the calculation of the area ratio between the YAG:Ce^{3+} particles and the TiO_2 film.

Fig. 6 shows the cross-sectional morphology of the pure TiO_2 film and the compounded TiO_2 film. The thicknesses of both films are about 6–8 μm. The films exhibit a well adhesion with the substrate without any discontinuity at the interface. For the compounded film, a few YAG:Ce^{3+} particles were observed, which indicated that the YAG:Ce^{3+} particles also existed inside the film. Obviously, the YAG:Ce^{3+} particles have no effect on the TiO_2 film formation.

Fig. 7 illustrates the XRD patterns of the pure TiO_2 film and the compounded film. It reveals that the films consist of a large amount of anatase TiO_2 with a few rutile TiO_2. It was found that the full width at the half-maximum (FWHM) for the anatase peaks, located at 25.3°, are remarkably different from both films. According to Scherrer's formula, the grain size of pure TiO_2 is about 20–21 nm, while the compounded film is 13–14 nm, which suggests that the YAG:Ce^{3+} particles played a role as a nuclear seeds to reduce the grain size during the film oxidation. Therefore, the compounded film exhibits a smaller grain size than that of pure TiO_2 film. Due to the existence of the small amount of compound, no YAG peak appears in the XRD spectra.

Generally, the "*in situ*" growth of the TiO_2 film on the Ti alloy substrate using MAO includes the following processes. At the initial stage, CO_3^{2-} in aqueous electrolyte is ionized:

$$CO_3^{2-} + H_2O \rightarrow HCO_3^- + OH^-$$

Then, OH^- transfers towards the anode then react with Ti^{4+} on the surface of the substrate during MAO [19]:

$$Ti^{4+} + 2OH^- + 2H_2O \rightarrow TiO_2 + 2H_3O^+$$

Due to the high temperature and upper voltage caused by discharge sparks, Ti^{4+} from the substrate and OH^- in the electrolyte combine and form molten TiO_2. Simultaneously, the molten TiO_2 erupts from the discharge channels. At last, the morphology of craters and pores is shaped by quenching of electrolyte with a high cooling rate of 10^8 K/s [13].

There are three crystalline structures for TiO_2, including anatase, rutile and brookite [9]. Generally speaking, only anatase TiO_2 exhibits superior photocatalytic activity. It has been known that TiO_2 crystal structure can be controlled by adjusting the parameters, such as voltage, duty cycle and oxidation time during MAO [14]. In this experiment, anatase phase, as shown in Fig. 7,

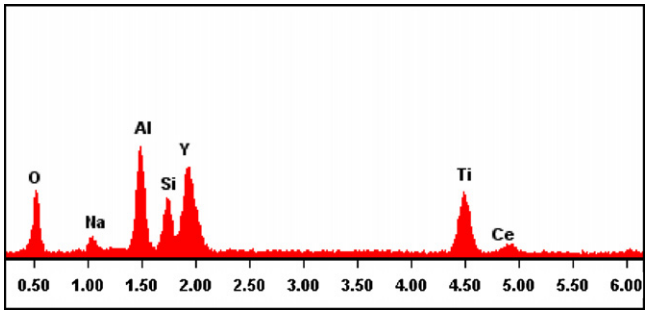

Fig. 5. EDS profile of the chemical compositions corresponding to point A in Fig. 4.

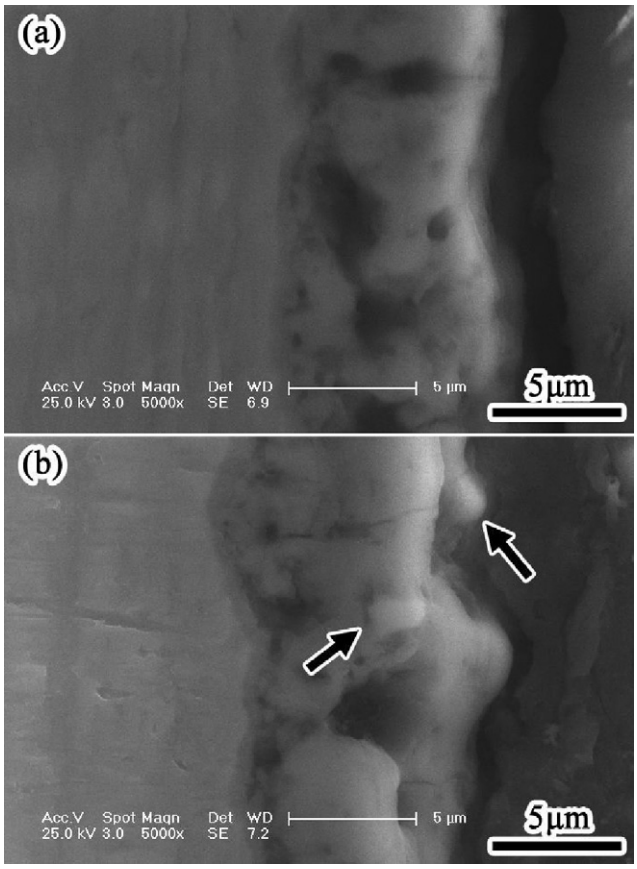

Fig. 6. Cross-section morphologies of TiO_2 films. (a) Without composites; (b) compounded with the YAG:Ce^{3+} (arrows indicate the YAG:Ce^{3+} particles).

in the TiO_2 film is expected to show desired photocatalytic properties.

When the YAG:Ce^{3+} powder was added into the electrolyte, it was homogeneously distributed under vigorous stirring. During MAO, when the molten TiO_2 erupted from the discharge channels, YAG:Ce^{3+} particles would be mixed within the TiO_2. Under high temperature from the molten TiO_2, the YAG:Ce^{3+} particles were melted partly and have a short-range diffusion around the interface. Therefore, the original YAG:Ce^{3+} polyhedron particles transformed into roundish particles in the TiO_2 film without obvious boundary between the YAG:Ce^{3+} particle and the TiO_2 substrate. In the YAG:Ce^{3+} particles, the rare earth metals with incompletely occupied 4f and empty 5d orbit could restrain the growth of TiO_2 crystalline [20], which makes the grain size much smaller. The heterojunction between the YAG:Ce^{3+} particle and the TiO_2 phase might provide a superior photocatalytic effect.

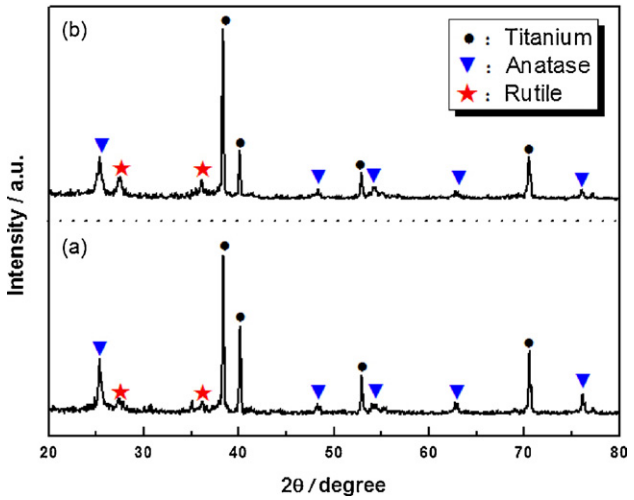

Fig. 7. XRD patterns of TiO_2 films. (a) Without composites; (b) compounded with the YAG:Ce^{3+}.

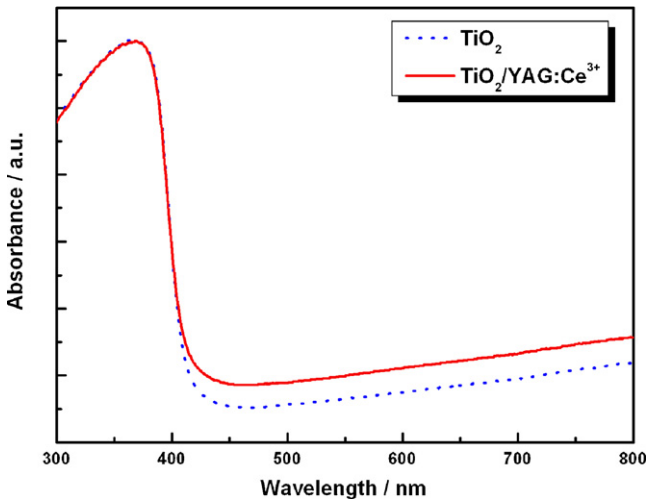

Fig. 8. UV–vis diffuse reflectance spectra (DRS) of pure TiO_2 and TiO_2/YAG:Ce^{3+} films.

3.2. Photocatalytic properties of the TiO_2 films

Fig. 8 illustrates the DRS profiles for the pure TiO_2 film and the TiO_2/YAG:Ce^{3+} film. Both traces reveal a high absorbance in ultraviolet light and the absorption edge occur at the wavelength of 420 nm. Comparing with the pure TiO_2 film, the TiO_2/YAG:Ce^{3+} compounded film shows a higher absorption over the wavelength of 400 nm. It is well known that YAG:Ce^{3+} is an important luminescent material and Ce^{3+} activated YAG exhibits strong absorbance in the blue light [17]. Therefore, the visible light absorbance was increased in the compounded film. However, the issue why the absorption is enhanced in the visible light still needs to be further studied in the future.

Photo-generated current test is an effective method to study the photo-induced charges separation efficiency of semiconductors. The intensity of illuminating light, the surface characters and the chemical compositions of the film remarkably affect the photo-generated current. When the light is on, the photons whose energies are larger than the bandgap are absorbed by the catalysis, which induce the electrons in valence band transit to conduction band and left holes in the valence band, and then the photocurrent is generated. Fig. 9 illustrates the photo-generated current intensity of both pure TiO_2 film and TiO_2/YAG:Ce^{3+} film irradiated by high pressure mercury lamp.

Obviously, the photo-generated current intensity of the TiO_2/YAG:Ce^{3+} film is almost 1.5 times larger than the pure TiO_2 film, which demonstrates that the YAG:Ce^{3+} composites exhibit a significant effect on increasing the concentration of the charge carriers. The multiple electron energy levels in Ce^{3+} helps to generate the carrier trapping center around the heterojunctions on the compounded film [20], thus extends the e^-/h^+ recombination period and reduces the recombination rate. Meanwhile, the larger specific surface area of the TiO_2/YAG:Ce^{3+} film also enhances the photo-generated current intensity.

Fig. 10 gives the photocatalytic efficiency of the TiO_2 films for degrading the methyl blue. A blank test (without any TiO_2 film)

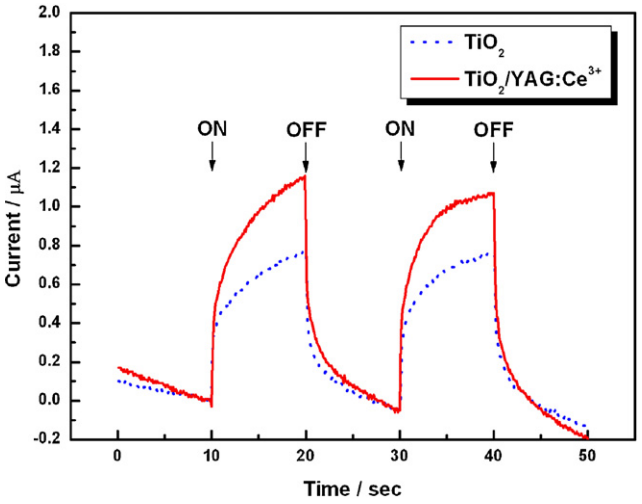

Fig. 9. Photo-generated current of pure TiO_2 and TiO_2/YAG:Ce^{3+} films.

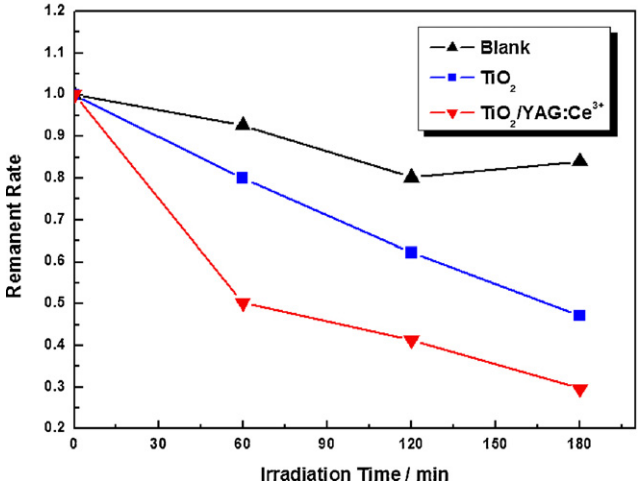

Fig. 10. The concentration of methyl blue photo-degraded by pure TiO_2 and TiO_2/YAG:Ce^{3+} films.

was employed which shows that only a small amount of methyl blue was decomposed. The concentration of methyl blue degraded by the pure TiO_2 film dropped to nearly 50%. The TiO_2/YAG:Ce^{3+} film shows the highest decomposition rate with the concentration dropped to 30%. These results further demonstrate that the TiO_2/YAG:Ce^{3+} film exhibits a superior photocatalytic property than that of the pure TiO_2 film due to its stronger absorption, higher concentration of charge carriers and larger specific surface area.

4. Conclusions

Micro-arc oxidation (MAO) provides a valid process for "*in situ*" preparing a photocatalytic film on the Ti alloy surface. It not only can control the percent of the crystal phase (anatase, rutile) of the TiO_2 film by adjusting the experimental conditions, but also achieve doped and compounded TiO_2 film through changing the chemical compositions in the electrolyte. Therefore, it is expected that MAO will be a simple, economic and promising approach to the preparation of superior photocatalytic TiO_2 film.

Acknowledgements

This research was financially supported by the National Basic Research Program of China (973 Program) (Nos. 2009CB939704 and 2009CB939705), the Nature Science Foundation of Hubei Province, China (No. 2007ABA217) and the Self-research Program for Doctoral Candidates (including Mphil-PhD) of Wuhan University in 2008 (No. 2008202020100000).

References

[1] A. Fujishima, K. Honda, Nature 238 (1972) 37–38.
[2] Y. Liao, W. Que, J. Alloys Compd. 505 (2010) 243–248.
[3] F.D. Fonzo, C.S. Casari, V. Russo, M.F. Brumella, A.L. Bassi, Nanotechnology 20 (2009) 15604–15610.
[4] J. He, Q.Z. Cai, Y.G. Ji, H.H. Luo, D.J. Li, B. Yu, J. Alloys Compd. 482 (2009) 476–481.
[5] O. Carp, C.L. Huisman, A. Reller, Prog. Solid State Chem. 32 (2004) 33–177.
[6] Y. Tu, S. Huang, J. Sang, X. Zou, J. Alloys Compd. 482 (2009) 382–387.
[7] D. Wu, M. Long, W. Cai, C. Chen, Y. Wu, J. Alloys Compd. 502 (2010) 289–294.
[8] X. Gao, W. Sun, Z. Hu, G. Ai, Y. Zhang, S. Feng, F. Li, L. Peng, J. Phys. Chem. C 113 (2009) 20481–20485.
[9] T.L. Thompson, J.T. Yates, Chem. Rev. 106 (2006) 4428–4453.
[10] K.Y. Jung, S.B. Park, Appl. Catal. B: Environ. 25 (2000) 249–256.
[11] H. Yang, C. Pan, J. Alloys Compd. 492 (2010) L33–L35.
[12] B. Liu, L. Wen, X. Zhao, Sol. Energy Mater. Sol. Cells 92 (2008) 1–10.
[13] A.L. Yerokhin, X. Nie, A. Leyland, A. Matthews, S.J. Dowey, Surf. Coat. Technol. 122 (1999) 73–93.
[14] M.R. Bayati, F. Golestani-Fard, A.Z. Moshfegh, Appl. Surf. Sci. 256 (2010) 4253–4259.
[15] X. Wu, Z. Jiang, H. Liu, S. Xin, X. Hu, Thin Solid Films 441 (2003) 130–134.
[16] X. Shi, Q. Wang, F. Wang, S. Ge, Min. Sci. Technol. 19 (2009) 220–224.
[17] Y. Zhou, J. Lin, M. Yu, S. Wang, H. Zhang, Mater. Lett. 56 (2002) 628–636.
[18] G. Feng, S. Liu, Z. Xiu, Y. Zhang, J. Yu, Y. Chen, P. Wang, X. Yu, J. Phys. Chem. C 112 (2008) 13692–13699.
[19] A.L. Yerokhin, A. Leyland, A. Matthews, Appl. Surf. Sci. 200 (2002) 172–184.
[20] X. Wu, W. Qin, X. Ding, Y. Wen, H. Liu, Z. Jiang, J. Phys. Chem. Solids 68 (2007) 2387–2393.